Materials Science & Engineering A 658 (2016) 484–489

Contents lists available at ScienceDirect

Materials Science & Engineering A

journal homepage: www.elsevier.com/locate/msea

Spatial Martensite

Arpan Das *

Fatigue and Fracture Group, Materials Science and Technology Division, CSIR - National Metallurgical Laboratory, Jamshedpur 831 007, Jharkhand, India[1]

ARTICLE INFO

Article history:
Received 26 November 2015
Accepted 24 January 2016
Available online 18 February 2016

Keywords:
Stress induced martensite
Strain induced martensite
Strain rate
Tensile test
Austenitic stainless steel

ABSTRACT

The spatial distribution of martensite laths at different strained austenite grains has been thoroughly investigated by strain rate variation during tensile deformation of metastable austenitic stainless steel at ambient temperature. Deformation induced martensitic transformation has been studied through direct measurement of martensite fraction and their distribution at various levels of stress/strain for different strain rates. The nature of distribution of martensite laths closely corresponds to the local *stress-state* and *strain-state* variation in a tensile deformed and fractured specimen. The martensite laths' distribution pattern is strongly attributed to the crystallographic nature of *variant selection* due to applied stress. It has also been investigated that the spatial distribution of martensite lath is strain rate dependent.

1. Introduction

Austenitic stainless steels are widely being preferred by chemical and nuclear power plant industries due to their good mechanical properties, outstanding corrosion resistance in a wide range of environments and good weldability. Metastable austenitic stainless steels are generally designed to be unstable thermodynamically so that martensitic transformation can take place due to externally applied load or temperature fluctuation. The deformation process can induce the formation of two types of martensites in austenitic stainless steels, where the first is ϵ (hcp) martensite and the second is α' (bcc) martensite. In case of solid-state phase transformation where concurrently there is a latent heat of transformation and adiabatic heat are generated inside the material due to plastic straining. The transformation sequences are generally reported and accepted to be: $\gamma(fcc) \rightarrow \epsilon(hcp)$, $\gamma(fcc) \rightarrow \epsilon(hcp) \rightarrow \alpha'(bcc)$, $\gamma(fcc) \rightarrow deformation\ \ twin \rightarrow \alpha'(bcc)$ and $\gamma(fcc) \rightarrow \alpha'(bcc)$ [1–4]. The nucleation sites of these deformation induced martensites (*DIM*) are generally reported to be: shear band intersections, isolated shear bands, grain boundary triple junctions, shear band-grain boundary intersections, and twin faults according to their interaction energy. This transformation is mainly affected by many parameters, such as: alloy composition, temperature, strain, stress, strain rate, grain size, initial texture and deformation mode [5]. The stacking fault energy (*SFE*) of austenite, as a function of the alloy composition and temperature, is the most important factor that controls the deformation micro-mechanisms, which has been critically reviewed and reported by the present author elsewhere [6].

The phenomenological theory of martensite crystallography gives the complete description of the mathematical link between the orientation relationship, habit plane and the shape deformation for each martensite lath that forms by displacive transformation [7]. While the most common application of this theory is to understand the martensitic transformation, the theory also finds application equally well for bainitic transformation [8]. It is well established that martensitic transformation can be triggered above the martensite start temperature (M_S) by the deformation of austenite. Considering that, mechanical driving force controls the *variant selection* process, the previous investigations revealed good agreement between measured pole figures and those calculated using Patel and Cohen's theory [9]. The thermodynamic effect of mechanical driving force acts as a key factor in controlling the deformation-induced martensitic transformation from metastable austenite [8–10].

The microstructure descriptions based only on fractions of martensite lath's populations are an incomplete description. The extent, number, shape, size, aspect ratio and the nature of distribution of martensite laths evolved during deformation in polycrystalline materials is extremely important for designing the structural components. It is generally accepted that martensite is nucleated heterogeneously, *i.e.*, that the virgin austenite contains embryos which become operative and grow into macroscopic plates when the driving force is sufficiently large. The purpose of the present investigation is to evaluate quantitatively the spatial distribution of α' (bcc) martensite laths in different strained

* Present address: Mechanical Metallurgy Division, Materials Group, Bhabha Atomic Research Centre (Department of Atomic Energy), Trombay, Mumbai 400 085, Maharashtra, India.
E-mail address: dasarpan1@yahoo.co.in
[1] Research conducted.

http://dx.doi.org/10.1016/j.msea.2016.01.072
0921-5093/

austenite grains under tensile deformation at various strain rates under ambient temperature.

2. Experimental

Nuclear grade *AISI* 304*LN* metastable austenitic stainless steel has been chosen for the present study. Chemical composition (in wt.%) of the material is: C 0.03, Mn 1.78, Si 0.65, S 0.02, P 0.034, Ni 8.17, Cr 18.73, Mo 0.26, Cu 0.29, N 0.08 and the balance Fe. SEM micrograph shown in Fig. 1(a) reveals that in the as-received condition, the microstructure of the investigated steel consists of polygonal grains of austenite with annealing twins, characteristic of austenitic stainless steels, interspersed in some grains. The M_{d30} temperature of the material at which 50% of the austenite transforms to martensite at a true strain of 0.30, calculated from the equation of Angel [11], is found to be $\approx 2.8\,^{\circ}C$. Initial austenite grain size of the material was found to be ≈70 μm. The mechanical properties of *AISI* 304*LN* stainless steel at five different strain rates (*i.e.*, 1.0, 0.1, 0.01, 0.001 and 0.0001 s^{-1}) have been determined through tensile tests of cylindrical solid specimens at ambient temperature (Fig. 1(b and c)). Low temperature tensile properties of the same alloy at various strain rates are also reported by Barat et al. [12] elsewhere.

One half of all the fractured tensile specimens (room temperature specimens) were longitudinally sectioned along the mid-plane, mounted (Fig. 1 (d)), polished and etched with a mixture of HCl and HNO_3 in 2:1 ratio. Few drops of C_2H_5OH were used to reveal the martensite laths under optical microscope (Fig. 1(e and f)). Various techniques (*i.e.*, *EBSD*, *XRD*, *TEM*, Image Processing, and magnetic measurement) are generally used to determine the extent of austenite transforming to martensite. Image processed micrograph is shown in Fig. 1(f).

For investigating the nucleation sites for deformation-induced phase transformation and to understand the mechanisms of evolution of martensites, thin discs of 2.0 mm thickness were extracted from uniformly deformed (room temperature) regions of the tested specimens using a slow speed cutter, and the discs were mechanically thinned down to 0.10 mm thickness using increasingly finer grades of grit paper. Following mechanical polishing, 3.0 mm diameter discs were extracted from the thinned discs using a punching apparatus, and subsequently thinned in a twin-jet electro polisher using 9:1 acetic-perchloric acid mixture at 45 V until perforation. The perforated thin foils were examined under *TEM* in a double tilt holder at an operating voltage of 200 kV.

In the present research, extensive Image Processing has been carried out on the etched optical micrographs obtained from cross-sectional planes (shown in Fig. 1(d)) along the specimen axis and parallel to the fracture surface for quantitative information on spatial martensite (at various stresses/strains) in specimens tested at different strain rates. Starting from the fracture end of the specimens, a large number of optical images were sequentially viewed under an optical microscope at predetermined diametral locations (at different stresses/strains), and images of the microstructure were digitally recorded with a magnification of 400X. Martensite appears darker in the bright background of matrix austenite under the optical microscope (Fig. 1(e and f)). These optical images were analysed after appropriate grey-thresholding to obtain the area fraction of martensite as a function of true plastic strain (Fig. 1(f)).

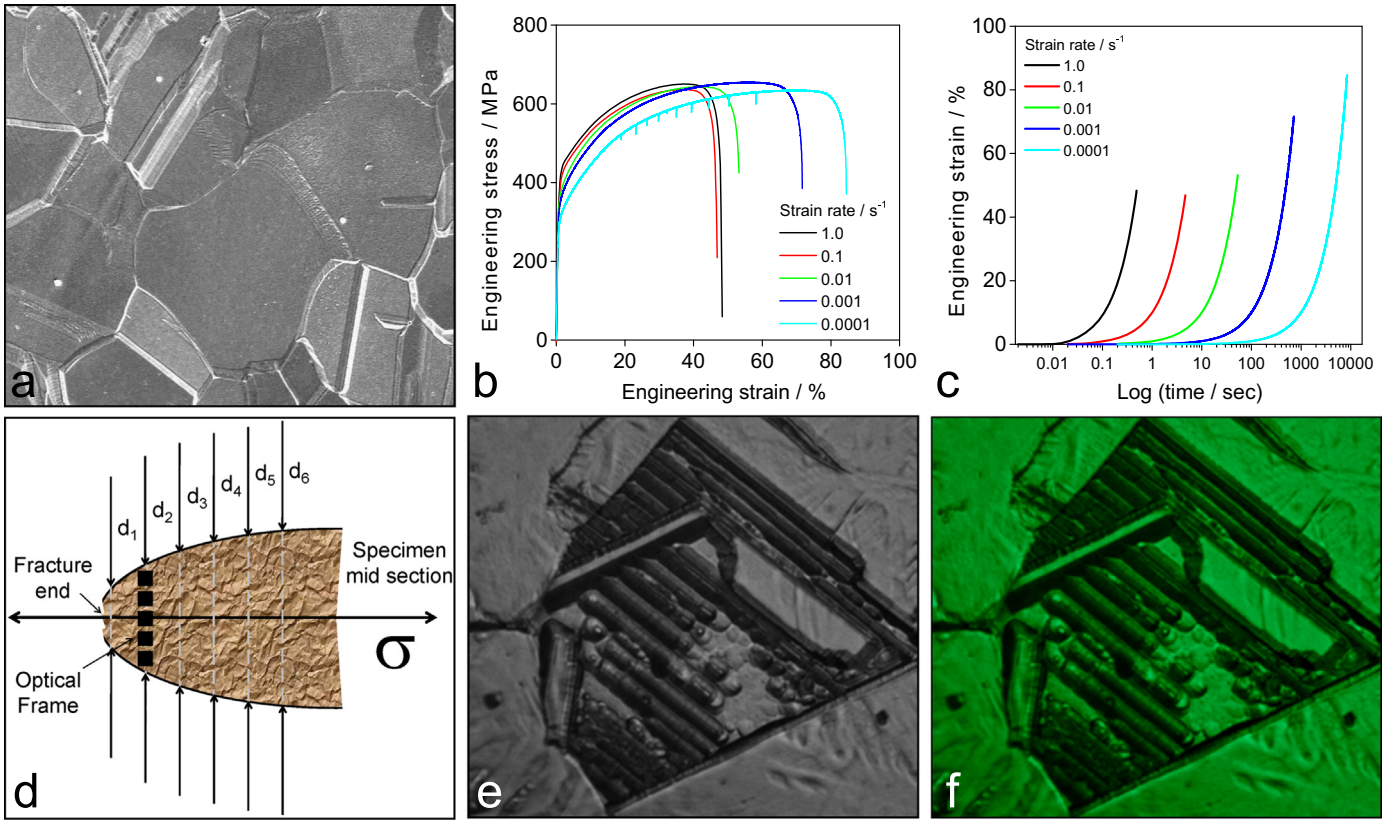

Fig. 1. (a) *SEM* microstructure of *AISI 304LN* stainless steel showing metastable polygonal austenitic grains and annealing twins, (b) Engineering stress–engineering strain curve [1,2] and (c) engineering strain–time curve tested at ambient temperature with various strain rates, (d) Schematic of metallographic sample inside the mould for quantifying *DIM* volume fraction at various stress/strain levels, (e) Optical microstructure of deformed *AISI* 304*LN* stainless steel showing DIM laths (*i.e.*, black colour) and (f) after image processed: DIM (black) and austenite (green). (For interpretation of the references to color in this figure caption, the reader is referred to the web version of this paper.)